Acta Crystallographica Section D
**Biological Crystallography**
ISSN 0907-4449

# Mass-spectrometry assisted heavy-atom derivative screening of human Fc$\gamma$RIII crystals

**Peter D. Sun[a]* and Carl H. Hammer[b]**

[a]Structural Biology Section, National Institute of Allergy and Infectious Diseases, The National Institutes of Health, 12441 Parklawn Drive, Rockville, Maryland 20852, USA, and [b]Research Technology Branch, National Institute of Allergy and Infectious Diseases, The National Institutes of Health, 12441 Parklawn Drive, Rockville, Maryland 20852, USA

Correspondence e-mail: psun@nih.gov

Received 11 October 1999
Accepted 23 November 1999

A heavy-atom screening method aided by mass spectrometry is described here. Using mass spectrometry, several heavy-atom compounds have been screened in order to obtain potential phasing derivatives for the crystals of a human immunoglobulin Fc receptor, Fc$\gamma$RIII. Of these, $HgCl_2$, trimethyllead acetate (TMLA), $KAu(CN)_2$, $K_2PtCl_4$ and $PbAc_2$ reacted with Fc$\gamma$RIII in solution, whereas $KAuCl_4$, ethylmercuric thiosalicylate (EMTS) and $Na_2WO_4$ did not. To validate the mass-spectrometry results, these heavy-atom compounds were also used to soak crystals of Fc$\gamma$RIII and crystallographic data were collected after soaking. The calculated $R_{iso}$ indicated that $HgCl_2$, TMLA, $K_2PtCl_4$ and $PbAc_2$ were likely to form derivatives, whereas $KAu(CN)_2$ and $Na_2WO_4$ were not. The anomalous difference Patterson maps calculated for the $HgCl_2$ and TMLA derivative data sets were of good quality and can readily be interpreted by hand. In general, the number of binding sites obtained from the crystallographic phase refinement of the derivatives agrees with those obtained from the mass spectrometry, suggesting that mass spectrometry can be applied for rapid searching of suitable heavy-atom derivatives for X-ray crystallography.

## 1. Introduction

As direct methods are yet to be improved, the predominant methods of phasing protein diffraction data to date are either isomorphous replacement or molecular-replacement methods. In many determinations of new protein structures, phasing by heavy-atom derivatization is still the method of choice. However, one of the difficulties associated with the heavy-atom based phasing is the process of finding a suitable heavy-atom derivative. The conventional heavy-atom screening method is not only an empirical process but is often also a lengthy process that requires the acquisition of multiple diffraction data sets. In recent years, the development of the selenomethionine (SeMet) based multiwavelength anomalous dispersion (MAD) method in protein phasing has overcome the cumbersome process of heavy-atom screening (Hendrickson, 1991). The primary advantage of SeMet phasing over the conventional heavy-atom screening method derives from the ability of the SeMet method to provide a heavy-atom derivative with certainty without having to go through the uncertain and lengthy screening process. Other means of generating heavy-atom derivatives without implementing a screening process have also been used in the past, such as introducing cysteine mutations (Dao-pin *et al.*, 1987) and utilizing known heavy-metal cofactors of the native structure (Zhang *et al.*, 1995).

Owing to its high accuracy in molecular mass determination, mass spectrometry has become a very useful tool for protein crystallography in general and particularly in characterizing a protein preparation or identifying proteolytic fragments (Chait, 1994). Occasionally, mass spectrometry has also been applied to validate heavy-metal derivatives (Krishna *et al.*, 1994). Here, we attempted to replace the conventional heavy-atom screening with a mass-spectrometry assisted heavy-atom screening in order to identify suitable derivatives of an Fc$\gamma$ receptor crystal. The potential pitfalls associated with a conventional heavy-atom screening method, such as the need to collect multiple trials of heavy-atom data sets, are avoided. Instead, the preliminary heavy-atom compounds are screened in solution and characterized using mass spectrometry. The method not only enables a rapid selection and optimization of the potential derivatives, but also limits the use of crystals.

## 2. Materials and methods

### 2.1. Protein expression and purification

The extracellular ligand-binding domain of human Fc$\gamma$RIII, residues 1–172 of the mature sequence, was subcloned into a Novagen pET-28b vector using the *Nco*I and *Not*I restriction sites and the BL21(DE3) strain of *Escherichia coli*. To facilitate the expression and purification, Met-Ala was added to the 5′ end of the gene and a histidine tag (Ala-Ala-Ala-Leu-Glu-$His_6$) was added to the 3′ end. The expression construct for the natural killer receptor KIR2DL2 has been described elsewhere (Snyder *et al.*, 1999). The protein was first expressed in inclusion-body form and then reconstituted *in vitro*. In brief, cells containing the Fc$\gamma$RIII-expressing plasmid were grown in a 10 l Newbrunswick Bioflo 3000 bio-reactor vessel and induced with 0.5 m*M* IPTG at an approximate $OD_{595}$ of 10.0 for 5 h. Once harvested, the inclusion bodies were isolated by repeated washing with 2 *M* urea solution and then redissolved in 8 *M* urea prior to refolding. The refolding reaction was initiated by a rapid dilution of the urea-dissolved inclusion bodies of Fc$\gamma$RIII into a refolding buffer consisting of 0.5 *M* L-arginine, 5 m*M* $CaCl_2$, 10 µg ml$^{-1}$ AEBSF, 5 m*M* cystamine, 5 m*M* cysteamine, 50 m*M* Tris pH 8.0 and then dialyzing thoroughly against water. The renatured Fc$\gamma$RIII was concentrated on an Ni-affinity column and further purified on a HR10/30 Superdex 200 (Amersham Pharmacia Biotech) size-exclusion column.

### 2.2. Mass-spectrometry measurement of the derivatized Fc$\gamma$RIII protein

Electrospray ionization mass spectrometry (ESI–MS) measurements were acquired and recorded with a Perkin–Elmer Sciex API-300 triple quadruple system (Thornhill, Ontario, Canada), using a pneumatically assisted ion electrospray source. The mass spectrometer has a charge-to-mass ratio range of 30–3000. ESI measurements were acquired in positive-ion mode. Multiple charged ions were generated by spraying the solution through a stainless steel capillary held at 4450 V. Protein samples containing only volatile buffer and at a concentration of 10 pmol µl$^{-1}$ or greater were analyzed by direct infusion. An infusion pump (Model 200 Series, KD Scientific, Inc., Boston, MA) was used to deliver the sample in a carrier solution of 50% acetonitrile and 1% acetic acid at 5 µl min$^{-1}$ to the sprayer through a fused silica capillary of 100 µm internal diameter. When necessary, protein solutions were prepared by rapid on-line desalting through a protein trap cartridge (Michrom BioResources, Inc., Auburn, CA) placed in the injector loop of a 140C HPLC Microgradient System (Applied Biosystems, Foster City, CA) or in ports #6 and #9 of a two-position ten-port valve injector (Valco Instruments Co., Inc., Houston, TX). Step elution with 50% acetonitrile and 1% acetic acid at 20 µl min$^{-1}$ was used to deliver a concentrated and desalted analyte solution to the sprayer. The instruments' mass filters were calibrated and performance was verified to unit mass resolution (peak widths of $0.7 \pm 0.1$ Da at half height) using the singly charged poly(propylene glycols) (PPGs) supplied by PE-Sciex.

The protein samples for mass-spectrometry measurements were prepared by adding 0.5–1 µl of pre-dissolved heavy-atom compound solutions at various concentrations to 5–10 µl Fc$\gamma$RIII at 2–5 mg ml$^{-1}$ concentration in water. The derivatization reaction was allowed to proceed for 30 min at room temperature before infusion of the sample into the mass spectrometer.

### 2.3. Crystallization and X-ray crystallographic data collection

Crystals of Fc$\gamma$RIII were grown by hanging-drop methods with 10% PEG 4000, 50 m*M* Na HEPES at pH 7.0 and a protein concentration of approximately 7 mg ml$^{-1}$. Crystals grew to dimensions of $0.1 \times 0.2 \times 0.5$ mm in about one month. All X-ray diffraction data were collected on the Brookhaven NSLS X9B beamline under cryoconditions (93 K) and were processed using *HKL*2000 (Otwinowski & Minor, 1997). The heavy-atom derivative crystals were prepared by soaking heavy-atom compounds into the crystals. The heavy-atom binding sites were determined both by inspection of the difference Patterson maps or by using the *SHELX* program (Sheldrick, 1990). The heavy-atom refinement and phasing statistics were calculated using *PHASES* (Furey & Swaminathan, 1997).

## 3. Results

### 3.1. A test case

Previous crystallographic studies on the crystals of KIR2DL2, the extracellular ligand-binding domain of a natural killer cell surface receptor, have identified $KAu(CN)_2$ as a heavy-atom derivative with a phasing power of 1.4 to 3.4 Å resolution (Snyder *et al.*, 1999). To test whether the derivatization of KIR2DL2 can be revealed by the mass-spectrometry method, two reactions with molar concentration ratios $KAu(CN)_2$:KIR2DL2 of 9:1 and 28:1 were carried out in solution. Approximately 6.5 µg of KIR2DL2 protein was used in each reaction. The reactions were allowed to proceed for

**Table 1**
Mass-spectrometry measurement of KIR2DL2 and its $KAu(CN)_2$ derivative.

| Compound | Label | MS MW† | Diff. MW‡ | Calc. MW§ | Binding sites |
|---|---|---|---|---|---|
| Native | | 22226.0 | | 22228.0 | |
| $KAu(CN)_2$ | | 22226.0 | | | |
| | 1 | 22472.0 | 246 | 249 | 1 $Au(CN)_2^-$ |
| | 2 | 22720.8 | 495 | 498 | 2 $Au(CN)_2^-$ |
| | 3 | 22993.8 | 768 | 747 | 3 $Au(CN)_2^-$ |
| | 4 | 23223.9 | 998 | 996 | 4 $Au(CN)_2^-$ |
| | 5 | 23471.1 | 1245 | 1245 | 5 $Au(CN)_2^-$ |
| $KAu(CN)_2$ | | 22228.0 | | | |
| | 1 | 22472.0 | 244 | 249 | 1 $Au(CN)_2^-$ |
| | 2 | 22724.8 | 497 | 498 | 2 $Au(CN)_2^-$ |
| | 3 | 22972.3 | 744 | 747 | 3 $Au(CN)_2^-$ |
| | 4 | 23222.1 | 994 | 996 | 4 $Au(CN)_2^-$ |
| | 5 | 23473.5 | 1245 | 1245 | 5 $Au(CN)_2^-$ |

† MS MW, mass-spectrometry molecular weight. ‡ Difference molecular weight between the labeled peak and the native. § Calculated molecular weight of $Au(CN)_2^-$ is 249.

30 min and the samples were then analyzed by electrospray mass spectrometry (Fig. 1). The $KAu(CN)_2$-reacted KIR2DL2 protein resulted in five new peaks in addition to the diminished native peak (Figs. 1*a*, 1*b* and Table 1). The molecular mass of the native KIR2DL2 protein alone is 22 226 ± 2 Da, in agreement with the predicted molecular mass of 22 228 Da (Fig. 1*c*). The interval between these new derivative peaks agrees well with the calculated molecular weight of the gold adduct $Au(CN)_2^-$, thus reflecting the successive addition of gold cyanide to the protein. The five $Au(CN)_2^-$ adducts observed in mass spectrometry suggest that there are five potential gold cyanide binding sites in KIR2DL2. Subsequent

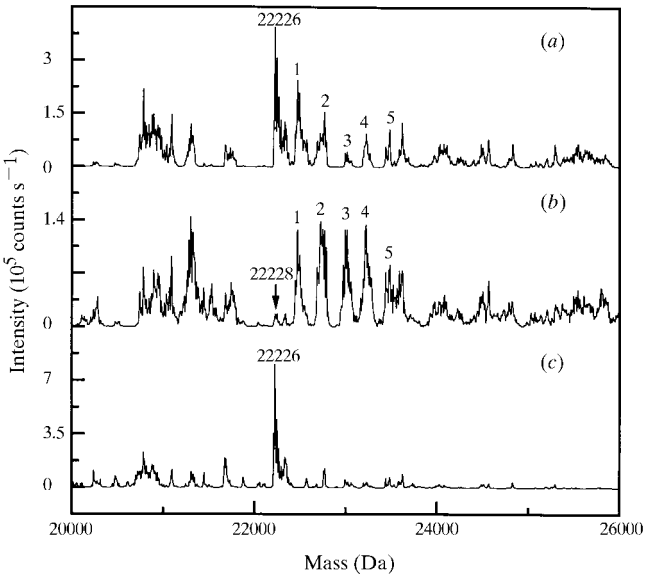


**Figure 1**
ESI–MS results of the gold cyanide reacted KIR2DL2 protein. The $KAu(CN)_2$ derivatization reaction was performed at [heavy atom]:[protein] molar ratios of 9:1 (*a*) and 28:1 (*b*). The $KAu(CN)_2$-derivatized peaks are labeled 1–5. The native untreated KIR2DL2 has a molecular weight of 22 226.0 Da (*c*).

**Table 2**
Mass-spectrometry measurements of Fc$\gamma$RIII with and without phosphate.

| Compound | Phosphate | MS MW | Diff. MW | Calc. MW† | Binding sites |
|---|---|---|---|---|---|
| Fc$\gamma$RIII | + | 20999.0 | | | |
| | | 21097.0 | 98 | 98 | 1 $H_3PO_4$ |
| | | 21194.0 | 195 | 196 | 2 $H_3PO_4$ |
| | | 21293.0 | 294 | 294 | 3 $H_3PO_4$ |
| | | 21390.0 | 391 | 392 | 4 $H_3PO_4$ |
| | | 21488.0 | 489 | 490 | 5 $H_3PO_4$ |
| | | 21586.0 | 587 | 588 | 6 $H_3PO_4$ |
| | − | 21001.0 | | | |

† The calculated molecular weight of $H_3PO_4$ is 98.

heavy-atom phase refinement of the $KAu(CN)_2$ derivative data resulted in five gold-binding sites (Table 5). Of the two $KAu(CN)_2$ reactions, the reaction with a 28:1 molar ratio of gold cyanide to native clearly resulted in a higher derivative peak intensity than did the 9:1 molar ratio reaction, indicating a correlation between the mass-spectrometry peak intensity and the extent of the heavy-atom reaction.

### 3.2. Fc$\gamma$RIII sample preparation

The sample of Fc$\gamma$RIII was prepared by *in vitro* reconstitution of the bacterium-expressed inclusion-body form of the protein, purified by an Ni-affinity HR10/30 Superdex 200 (Amersham Phamacia Biotech) gel-filtration column to homogeneity and dialyzed against water to a final concentration of 2–7 mg $ml^{-1}$.

### 3.3. Mass spectrometry of native Fc$\gamma$RIII: the binding of phosphate ions

A series of mass-spectrometry peaks, starting at a molecular weight of 20 999 ± 2 Da and spaced at approximately 98 Da intervals, were found when the native Fc$\gamma$RIII (6 mg $ml^{-1}$) sample was analyzed (Fig. 2*a*, Table 2). The main peak of 20 999 Da agrees well with the predicted molecular weight of

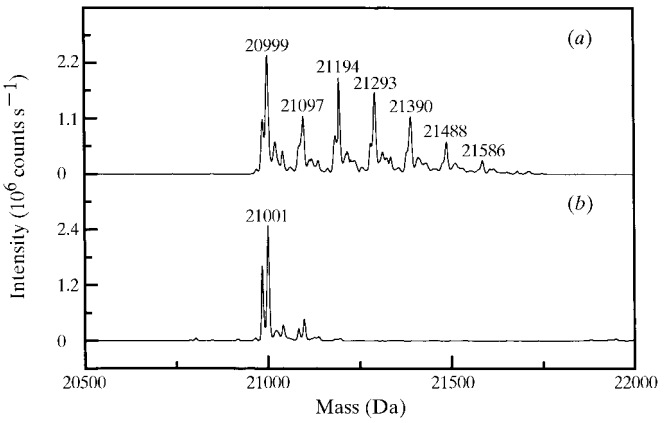


**Figure 2**
Native spectrum of Fc$\gamma$RIII. The protein samples were reconstituted (*a*) in the presence and (*b*) in the absence of a phosphate buffer. The native phosphate-free Fc$\gamma$RIII resulted a peak at a molecular weight of 21 001 Da.

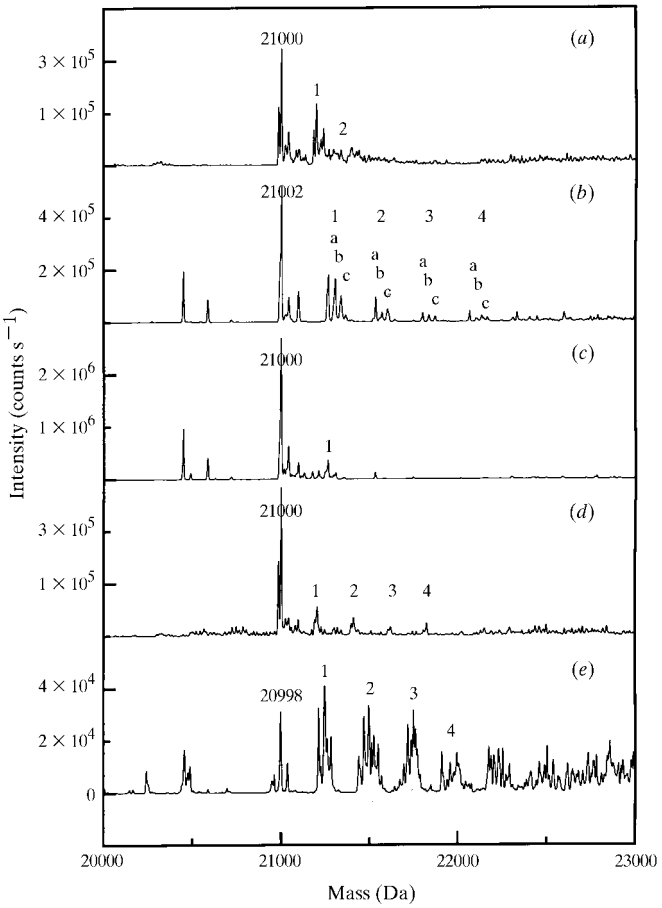


**Figure 3**
Mass spectrometry of Fc$\gamma$RIII reacted with (*a*) $HgCl_2$, (*b*) $K_2PtCl_4$, (*c*) TMLA, (*d*) $PbAc_2$ or (*e*) $KAu(CN)_2$. The molecular weight of the residual native peak is labeled in each panel. All derivative peaks are labeled in numeric order and are listed in Table 3.

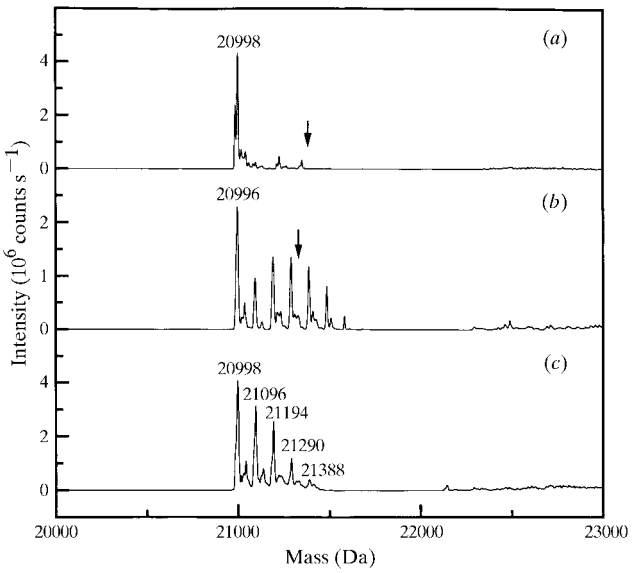


**Figure 4**
Mass spectrometry of (*a*) the EMTS-reacted and (*b*) the $KAuCl_4$-reacted Fc$\gamma$RIII, as well as the native (*c*). The arrow in each panel indicates the calculated molecular weight of Fc$\gamma$RIII with one heavy atom bound.

**Table 3**
Mass-spectrometry measurements of heavy-atom derivative reactions of Fc$\gamma$RIII.

| Name | Conc.† (mg ml$^{-1}$) | No. | MS MW | Diff. MW | Calc. MW‡ | Binding sites |
|---|---|---|---|---|---|---|
| Native | | | 21000 | | 20996 | |
| $HgCl_2$ | 5 | | 21000 | | | |
| | | 1 | 21198 | 198 | 200 | 1 $Hg^{2+}$ |
| | | 2 | 21398 | 398 | 400 | 2 $Hg^{2+}$ |
| $K_2PtCl_4$ | 10 | | 21002 | | | |
| | | 1*a* | 21266 | 264 | 266 | 1 $PtCl_2$ |
| | | 1*b* | 21304 | 302 | 301.5 | 1 $PtCl_3^-$ |
| | | 1*c* | 21336 | 334 | 337 | 1 $PtCl_4^{2-}$ |
| | | 2*a* | 21534 | 532 | 532 | 2 $PtCl_2$ |
| | | 2*b* | 21568 | 566 | 567.5 | 1 $PtCl_2$ + 1 $PtCl_3^-$ |
| | | 2*c* | 21600 | 598 | 603 | 1 $PtCl_2$ + 1 $PtCl_4^{2-}$ |
| | | 3*a* | 21798 | 796 | 798 | 3 $PtCl_2$ |
| | | 3*b* | 21834 | 832 | 833.5 | 2 $PtCl_2$ + 1 $PtCl_3^-$ |
| | | 3*c* | 21870 | 868 | 869 | 2 $PtCl_2$ + 1 $PtCl_4^{2-}$ |
| | | 4*a* | 22064 | 1062 | 1064 | 4 $PtCl_2$ |
| | | 4*b* | 22100 | 1098 | 1099.5 | 3 $PtCl_2$ + 1 $PtCl_3^-$ |
| | | 4*c* | 22134 | 1132 | 1135 | 3 $PtCl_2$ + 1 $PtCl_4^{2-}$ |
| $K_2PtCl_4$ | 10 | | 21001 | | | |
| | | 1 | 21301 | 300 | 301.5 | 1 $PtCl_3^-$ |
| | | 2 | 21601 | 600 | 603 | 2 $PtCl_3^-$ |
| | | 3 | 21832 | 831 | 833.5 | 2 $PtCl_2$ + 1 $PtCl_3^-$ |
| TMLA | 40 | | 21000 | | | |
| | | 1 | 21250 | 250 | 252 | 1 $(CH_3)_3Pb^+$ |
| $PbAc_2$ | 40 | | 21000 | | | |
| | | 1 | 21204 | 204 | 207 | 1 $Pb^{2+}$ |
| | | 2 | 21409 | 408 | 414 | 2 $Pb^{2+}$ |
| | | 3 | 21618 | 618 | 621 | 3 $Pb^{2+}$ |
| | | 4 | 21822 | 822 | 828 | 4 $Pb^{2+}$ |
| $KAu(CN)_2$ | 10 | | 20998 | | | |
| | | 1 | 21246 | 248 | 249 | 1 $Au(CN)_2^-$ |
| | | 2 | 21496 | 498 | 498 | 2 $Au(CN)_2^-$ |
| | | 3 | 21750 | 752 | 747 | 3 $Au(CN)_2^-$ |
| | | 4 | 21995 | 997 | 996 | 4 $Au(CN)_2^-$ |
| EMTS | 10 | | 20998 | | | None |
| $KAuCl_4$ | 10 | | 20996 | | | None |

† Concentration of the heavy-atom solution used in the derivatization reaction. ‡ Calculated molecular weight from the chemical formula of the adducts. The calculated molecular weight for the heavy-atom ions are $PtCl_4^{2-}$, 337; $Hg^{2+}$, 200; $Pb^{2+}$, 207; trimethyllead [$(CH_3)_3Pb^+$], 252; $Au(CN)_2^-$, 249.

20 996 Da for Fc$\gamma$RIII. Since a $PO_4^{3-}$ ion and its different protonated forms give rise to molecular weights of 95–98 Da, it was suspected that the successive peaks observed in the mass spectrometry of the native Fc$\gamma$RIII represent $PO_4^{3-}$ ion adducts. A phosphate buffer was used during the reconstitution process of the receptor. To further investigate the existence of $PO_4^{3-}$ ions in this refolded sample, a refolding of Fc$\gamma$RIII was carried out in the absence of phosphate buffer with otherwise identical refolding and purification conditions. When this refolded sample was analyzed by mass spectrometry, only a single peak, the 21 001 Da peak, was evident in the spectrum (Fig. 2*b*). Thus, the multiple peaks observed in the native Fc$\gamma$RIII sample refolded in the presence of phosphate buffer represent different phosphate adducts of the

**Table 4**
X-ray data-collection statistics.

The derivatives listed here are mercuric chloride ($HgCl_2$), lead acetate ($PbAc_2$), trimethyllead acetate (TMLA), potassium platinum (II) tetrachloride ($K_2PtCl_4$) and sodium tungstate ($Na_2WO_4$).

| Data | λ (Å) | *a* (Å) | *b* (Å) | *c* (Å) | Resolution (Å) | $I/\sigma$ | $N_{ref}$ | Complete | $R_{sym}$† (%) | $R_{iso}$‡ |
|---|---|---|---|---|---|---|---|---|---|---|
| Native | 1.0402 | 78.9 | 147.8 | 36.4 | 2.30 (2.38–2.30) | 18.6 (4.3) | 19133 | 96.7 (90.0) | 4.3 (24.7) | |
| $HgCl_2$ | 1.0076 | 81.3 | 144.5 | 36.3 | 2.35 (2.43–2.35) | 16.1 (3.4) | 34036 | 98.8 (97.6) | 3.8 (25.1) | 0.208 |
| PbAc | 0.9497 | 78.4 | 144.3 | 36.3 | 2.5 (2.6–2.5) | 19.9 (8.5) | 28465 | 97.8 (94.2) | 3.7 (12.3) | 0.317 |
| TMLA | 0.9497 | 76.6 | 140.9 | 35.3 | 2.5 (2.6–2.5) | 15.9 (5.1) | 25328 | 99.3 (98.7) | 4.4 (18.6) | 0.147 |
| $K_2PtCl_4$ | 1.0704 | 79.6 | 146.2 | 36.3 | 2.7 (2.8–2.7) | 14.4 (4.6) | 22468 | 99.8 (98.7) | 5.2 (23.1) | 0.121 |
| $Na_2WO_4$ | 1.0212 | 79.1 | 146.6 | 36.4 | 2.7 (2.8–2.7) | 14.6 (4.1) | 19233 | 85.6 (78.3) | 5.1 (22.8) | 0.071 |
| $KAu(CN)_2$ | 1.0384 | 79.1 | 147.8 | 36.5 | 3.0 (3.11–3.0) | 10.8 (3.1) | 9479 | 56.5 (60.5) | 6.1 (26.8) | 0.032 |

† $R_{sym} = \sum|I_h - \langle I_h\rangle| / \sum I_h$, where $\langle I_h\rangle$ is the mean intensity of multiple measurements of symmetry-related reflections. ‡ $R_{iso} = \sum_h |F_{ph} - F_p| / \sum_h (F_p + F_{ph})$, where $F_{ph}$ and $F_p$ are the amplitudes of derivative and native data sets, respectively.

**Table 5**
Heavy-atom soaking of the Fc$\gamma$RIII crystals.

| | | | | | Phasing power | | | | |
|---|---|---|---|---|---|---|---|---|---|
| Derivative | Concentration | Soaking time | Binding sites (fractional coordinates) | Occupancy | $pp^{iso}$† | Res. (Å) | $pp^{ano}$† | Res. (Å) | FOM‡ |
| KIR2DL2 | | | | | | | | | |
| $KAu(CN)_2$ | 10 mg ml$^{-1}$ | 2 d | 0.637, 0.097, 0.242 | 1.00 | 2.09 | 3.6 | 2.15 | 3.6 | 0.54 |
| | | | 0.965, 0.642, 0.179 | 0.71 | | | | | |
| | | | 0.871, 0.225, 0.176 | 0.49 | | | | | |
| | | | 0.379, 0.576, 0.110 | 0.32 | | | | | |
| | | | 0.749, 0.680, 0.219 | 0.26 | | | | | |
| Fc$\gamma$RIII | | | | | | | | | |
| $HgCl_2$ | 0.5% saturated | 12 h | 0.104, 0.024, 0.367 | 1.00 | 1.94 | 3.0 | 2.67 | 2.6 | 0.55 |
| | | | 0.070, 0.048, 0.324 | 0.87 | | | | | |
| | | | 0.054, 0.042, 0.270 | 0.56 | | | | | |
| | | | 0.091, 0.037, 0.488 | 0.30 | | | | | |
| | | | 0.246, 0.010, 0.865 | 0.15 | | | | | |
| TMLA | 10 mg ml$^{-1}$ | 12 h | 0.432, 0.463, 0.263 | 1.00 | 1.77 | 3.0 | 2.84 | 2.6 | 0.54 |
| | | | 0.742, 0.299, 0.322 | 0.86 | | | | | |
| $K_2PtCl_4$ | 0.25 mg ml$^{-1}$ | 2 d | 0.847, 0.454, 0.699 | 1.00 | 1.93 | 3.0 | 3.07 | 2.6 | 0.56 |
| | | | 0.574, 0.542, 0.732 | 0.66 | | | | | |
| | | | 0.716, 0.690, 0.555 | 0.80 | | | | | |
| | | | 0.644, 0.359, 0.749 | 0.45 | | | | | |
| | | | 0.849, 0.463, 0.756 | 0.27 | | | | | |
| | | | 0.643, 0.555, 0.733 | 0.27 | | | | | |
| PbAc | 1.6 mg ml$^{-1}$ | 3 d | | | | | | | |
| $Na_2WO_4$ | 10 mg ml$^{-1}$ | 16 h | | | | | | | |
| $KAu(CN)_2$ | 5 mg ml$^{-1}$ | 36 h | | | | | | | |

† $pp^{iso}$ and $pp^{ano}$ are the phasing power for the isomorphous and anomalous components, respectively. ‡ FOM, figure of merit.

protein. The biological relevance of phosphate binding to the Fc receptor is not clear. However, the sites observed here are most likely the result of specific coordination rather than non-specific binding. Firstly, the phosphate buffer was introduced only at the inclusion-body dissolution step of the receptor refolding and would have been diluted to a negligible concentration (<1 n*M*) in the purified sample. This argues that the affinity of the phosphate binding would be better than nanomolar concentration. Secondly, at least one phosphate-binding site can be modeled into the electron-density map of the refined structure of Fc$\gamma$RIII.

### 3.4. Mass-spectrometry analysis of heavy-atom compound derivatized Fc$\gamma$RIII

Several heavy-atom compounds, including mercuric chloride, lead acetate, trimethyllead acetate (TMLA), platinum (II) tetrachloride, gold cyanide, gold chloride, ethylmercuric thiosalicylate (EMTS), iridium bromide and sodium tungstate, were screened for the formation of potential heavy-atom derivatives of Fc$\gamma$RIII. The derivatizing reactions were prepared with individual heavy-atom compounds dissolved in water at various concentrations (listed in Table 3). One complication in interpreting the Fc$\gamma$RIII mass-spectroscopic data is that the native Fc$\gamma$RIII often displays multiple peaks corresponding to phosphate adducts of the protein.

Two mercuric ion bound Fc$\gamma$RIII species, with molecular weights of 21 198 and 21 398 Da, were identified in addition to the unmodified 21 000 Da native species in the mass spectrum of the $HgCl_2$-derivatized protein sample (Fig. 3*a*, Table 3). The molecular-weight shifts of the derivatized forms are 198 and 398 Da, respectively. Compared with the calculated molecular weight of 200 for the $Hg^{2+}$ ion, these results suggest the two derivatized peaks correspond to one and two $Hg^{2+}$ ions bound to Fc$\gamma$RIII.

A series of platinum adducts were identified from the $K_2PtCl_4$-reacted Fc$\gamma$RIII spectrum (Fig. 3*b*). The molecular weights of each series (peaks within a series are denoted *a*, *b* and *c*) are consistent with a constant number of platinum ions associated with different numbers of chloride ions resulting from the binding of various platinum (II) chlorides (Table 3). All observed derivative peaks differ from the calculated molecular weights by one to four protons, which is well within the error range of the experiment. There are a total of four binding sites observed.

TMLA-derivatized Fc$\gamma$RIII resulted in a mass spectrum consistent with one $Pb(CH_3)_3^+$ ion being bound to the protein,

whereas the reaction with $PbAc_2$ yielded a spectrum consistent with four $Pb^{2+}$ ion binding sites (Figs. 3*c* and 3*d*). $KAu(CN)_2$ reactions resulted in up to four $Au(CN)_2^-$ ions bound to Fc$\gamma$RIII (Fig. 3*e*). In most of these cases, the intensity of the original underivatized form remains as the most prominent form, indicating sub-optimal reaction conditions. Further studies of concentration-dependent heavy-atom derivatization suggest that the intensity of the underivatized native form is inversely proportional to the concentration of heavy-atom reagent and the length of the reaction (data not shown).

No heavy-atom adducts were observed in the EMTS and $KAuCl_4$ reactions (Figs. 4*a* and 4*b*). The non-native peaks in both Figs. 4(*a*) and 4(*b*) can be interpreted as phosphate adducts. The expected molecular weights for EMTS and $KAuCl_4$, indicated by arrows in the figures, are 382 and 339 Da, respectively. Two other compounds, $Na_2WO_4$ and $IrBr_4$, resulted either in protein-sample aggregation or in non-specific binding, leading to the loss of the overall mass-spectrometry signal on reaction with Fc$\gamma$RIII (data not shown).

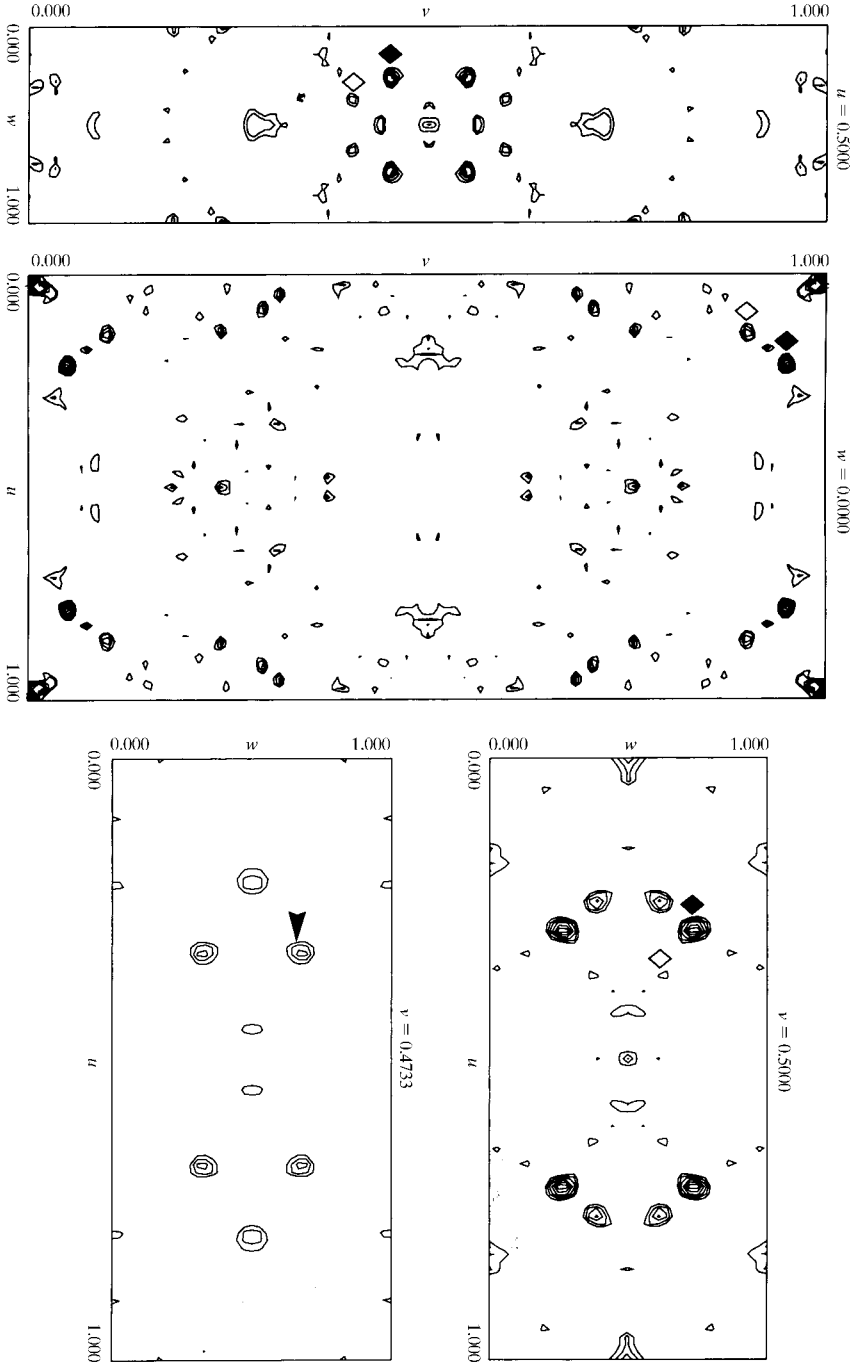


**Figure 5**
Three Harker sections ($u = 0.5$, $v = 0.5$ and $w = 0.0$) and a non-Harker section ($v = 0.4733$) of the $HgCl_2$ derivative anomalous difference Patterson map. The Harker peaks of the two highest occupancy sites, (0.104, 0.024, 0.367) and (0.070, 0.048, 0.324), are marked with filled and unfilled diamonds, respectively, and their cross peak is marked with an arrowhead at $v = 0.4733$.

### 3.5. X-ray data collection, $R_{iso}$ and anomalous Bijvoet Patterson map

Guided by the mass-spectrometry results of the heavy-atom derivatization reactions, crystals of Fc$\gamma$RIII were soaked in several heavy-atom solutions, as described in Table 5. Native crystals diffracted to 2.3 Å resolution and belong to space group $P2_12_12$, with unit-cell parameters $a = 78.9$, $b = 147.8$, $c = 36.4$ Å (Table 4). The calculated $V_m$ is 2.5, with two molecules in each asymmetric unit. Complete data sets were collected for $HgCl_2$-, $K_2PtCl_4$-, TMLA- and $PbAc_2$-soaked crystals and incomplete data were collected for $KAu(CN)_2$ and $Na_2WO_4$. The isomorphous difference, $R_{iso}$, calculated between the heavy-atom derivative data sets and the native data (Table 4), indicated the potential heavy-atom bindings for the $HgCl_2$, $K_2PtCl_4$, TMLA and $PbAc_2$ soakings, and the lack of derivatization for $KAu(CN)_2$ and $Na_2WO_4$ soakings. The anomalous Patterson maps calculated for the $HgCl_2$ and TMLA derivatives clearly indicated the degree of the derivatization (Figs. 5 and 6). The heavy-atom binding sites in the $HgCl_2$, TMLA and $K_2PtCl_4$ derivatives were readily interpreted either manually or by the program *SHELX* (Sheldrick, 1990).

### 3.6. Heavy-atom refinement and phasing statistics

The heavy-atom binding sites of the $HgCl_2$ and TMLA derivatives were further refined using the program suite *PHASES* (Furey & Swaminathan, 1997). Owing to the non-isomorphism among the deriva-

tive data sets, each derivative was refined separately against the native. The results of heavy-atom refinement indicate that all three derivatives ($HgCl_2$, TMLA and $K_2PtCl_4$) provide respectable heavy-atom phasing statistics (Table 5). The number of heavy-atom binding sites in the crystallographic asymmetric unit are five, two and six, respectively, for the $HgCl_2$, TMLA and $K_2PtCl_4$ derivatives.

### 3.7. Correlation between the crystallographic binding sites and mass spectrometry

The number of binding sites from the $KAu(CN)_2$-derivative phase refinement of KIR2DL2 compares well with that obtained from mass spectrometry (Table 6). In the case of Fc$\gamma$RIII, the number of heavy-atom binding sites derived from the heavy-atom phase refinement is approximately twice the number suggested by mass spectrometry. Since there are two molecules of Fc$\gamma$RIII in each crystallographic asymmetric unit, the actual number of binding sites per receptor molecule is half the number of total binding sites, which agrees well with the mass-spectrometry results.

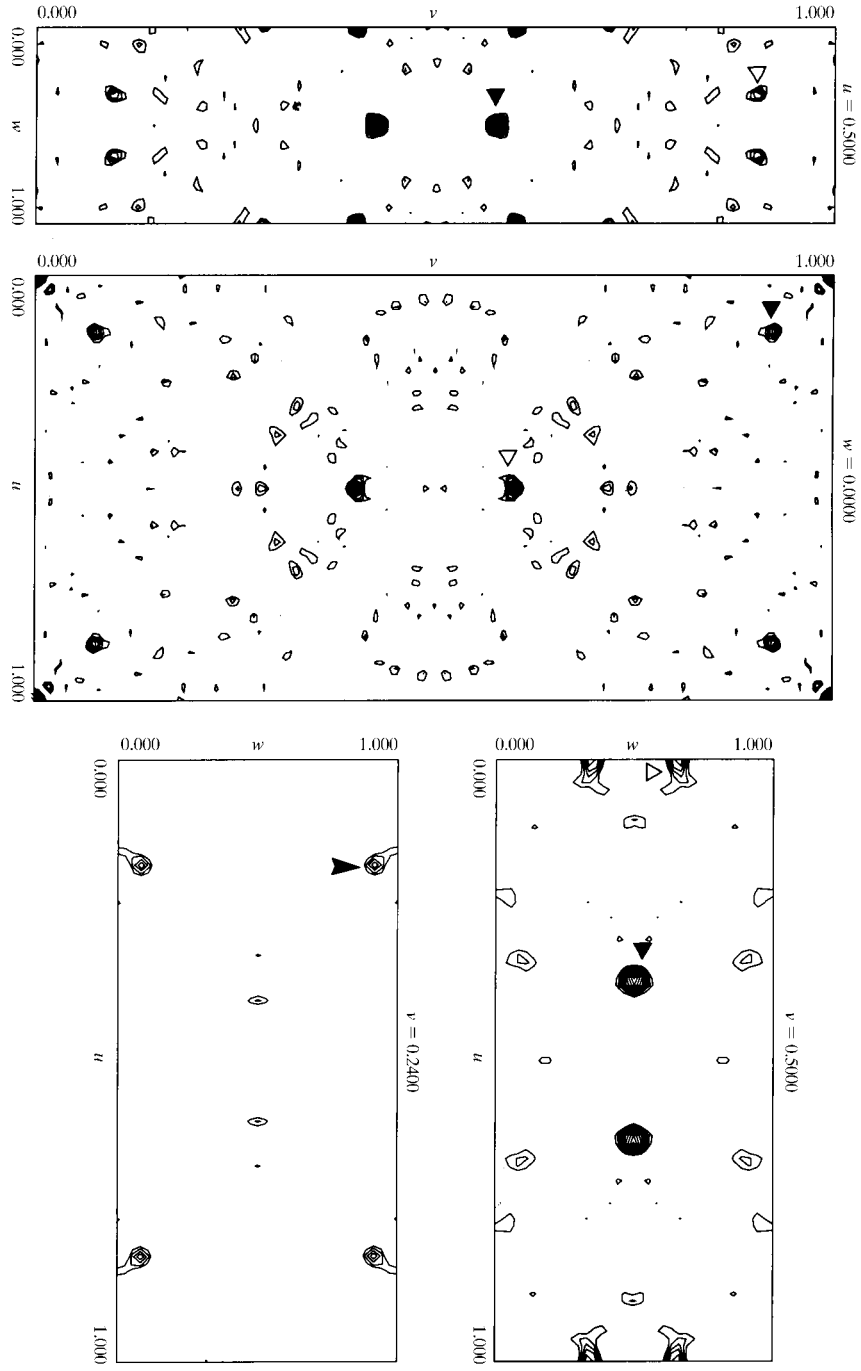


**Figure 6**
The corresponding Harker and non-Harker sections of TMLA derivative anomalous difference Patterson map. The Harker peaks are marked with filled and unfilled triangles for the two highest occupancy binding sites and their cross Patterson peak is marked with an arrowhead at $v = 0.2400$.

## 4. Discussion

In both the KIR2DL2 and Fc$\gamma$RIII cases, the results of heavy-atom derivatization obtained from mass spectrometry correlate with those obtained from crystallographic analysis in terms of number of binding sites. In some cases, such as in the $KAu(CN)_2$ derivative of KIR2DL2 and the $HgCl_2$ and $K_2PtCl_4$ derivatives of Fc$\gamma$RIII, even the occupancies of the heavy-atom binding sites obtained from the X-ray data correlate well with the relative intensities of the heavy-atom adducts from their respective mass spectra. Therefore, mass spectrometry can be used to indicate potentially useful heavy-atom derivatives for phasing diffraction data. It offers a rapid derivative-screening method, since there is no need to collect crystallographic data in the screening stage and a typical mass-spectrometry experiment takes only minutes to run instead of days for the acquisition of X-ray diffraction data. It helps to reduce the consumption of crystals for data collection by excluding unsuccessful heavy-atom compounds and including only the successfully derivatized heavy-atom compounds for data collection. This may be particularly important for situations in which data-collection-quality crystals are difficult to obtain. Furthermore, the method also opens the possibility of obtaining heavy-atom derivatives through co-crystallization in situations where soaking failed to generate derivatives yet successful derivatizations were observed through mass spectrometry in solution.

Although mass spectrometry is best for detecting covalent adducts to proteins, it is not uncommon for certain electrostatically

**Table 6**
Comparison between mass spectrometry and crystallographic results.

| Protein | Derivative | Number of sites | |
|---|---|---|---|
| | | X-ray | Mass spectrometry |
| KIR2DL2 | $KAu(CN)_2$ | 5 | 5 |
| Fc$\gamma$RIII | $HgCl_2$ | 5 | 2 |
| | TMLA | 2 | 1 |
| | $K_2PtCl_4$ | 6 | 4 |

bound ions to also be detected (Veenstra, 1999). For example, $Na^+$ and $Ca^{2+}$ ions are often found to be associated with proteins in mass spectrometry. In Fc$\gamma$RIII, up to six phosphate molecules are bound to the protein and give rise to multiple peaks spaced evenly at 98 Da intervals above the predicted native molecular weight. Thus, it is possible to use mass spectrometry to detect derivatives of electrostatic associations.

The soaking of crystals of Fc$\gamma$RIII in $KAu(CN)_2$ solution did not appear to achieve significant derivatization judging from the crystallographic $R_{iso}$ (Table 4), even though several heavy-atom binding sites were detected in the mass-spectrometry screening. This suggests that a heavy-atom compound may react differently in crystals compared with when it is in solution under slightly different conditions, particularly when the solubility of the heavy-atom compound is limited under the crystallization conditions. In this case, it may be more fruitful to obtain a derivatized crystal through co-crystallization with the heavy-atom compound. Indeed, co-crystallization of Fc$\gamma$RIII with $KAu(CN)_2$ has yielded a crystal with the same space group as that of the native. A complete data set collected from this crystal has an $R_{iso}$ of 0.108 (calculated on the amplitudes). At least one gold-binding site with full occupancy can be identified from a difference Fourier map; subsequent heavy-atom phase refinement resulted in a phasing power of 1.2 and a figure-of-merit of 0.46 for centric reflections.

A common problem in crystallographic heavy-atom soaking experiments is the determination of optimum crystal-soaking conditions. Using too concentrated heavy-atom solutions for soaking often compromises the X-ray diffraction, while too little heavy atom leads to inadequate derivatization. Often, several soakings of the same heavy-atom compound at different concentrations are carried out in order to obtain the optimum derivatization condition. With mass spectrometry, the minimum heavy-atom concentration required to achieve full derivatization can be defined. For example, when different concentrations of $KAu(CN)_2$ are reacted with KIR2DL2, the reaction with a 28:1 molar ratio of $KAu(CN)_2$ to KIR2DL2 resulted in a more complete derivatization than the 9:1 molar ratio reaction, judging from the residual intensity of the unreacted native form (Figs. 1*a* and 1*b*). In principle, other parameters governing a successful derivatization reaction, such as pH, salt and reaction time, can also be optimized using mass spectrometry. However, one should be aware that reactions in crystals may differ from those in solution owing to the presence of precipitation reagents and the restriction of diffusion by the crystal lattice.

We thank Dr Z. Dauter for help in using the X9B beamline at Brookhaven National Laboratory, Drs J. Boyington, C. Titlow, Mr G. Snyder and S. Motyka for their help in X-ray crystallographic data collection, Drs C. Sautes-Fridman and W. Fridman for supplying the Fc$\gamma$RIII plasmid DNA and Ms Ann Hanson for manuscript preparation. This work is funded by the intramural research of the National Institute of Allergy and Infectious Diseases, National Institutes of Health.

## References

Chait, B. T. (1994). *Structure*, **2**, 465–467.
Dao-pin, S., Alber, T., Bell, J. A., Weaver, L. H. & Matthews, B. W. (1987). *Protein Eng.* **1**, 115–123.
Furey, W. & Swaminathan, S. (1997). *Methods Enzymol.* **277**, 590–620.
Hendrickson, W. A. (1991). *Science*, **254**, 51–58.
Krishna, T. S. R., Fenyo, D., Kong, X.-P., Gary, S., Chait, B. T., Burgers, P. & Kuriyan, J. (1994). *J. Mol. Biol.* **241**, 265–268.
Otwinowski, Z. & Minor, W. (1997). *Methods Enzymol.* **276**, 307–326.
Sheldrick, G. (1990). *Acta Cryst.* A**46**, 467–473.
Snyder, G. A., Brooks, A. G. & Sun, P. D. (1999). *Proc. Natl Acad. Sci. USA*, **96**, 3864–3869.
Veenstra, T. D. (1999). *Biophys. Chem.* **79**, 63–79.
Zhang, G., Kazanietz, M. G., Blumberg, P. M. & Hurley, J. H. (1995). *Cell*, **81**, 917–924.